Japanese Journal of Structural Geology, No. 47, 23-36, 2003

Article

Deformation pattern of convergent margin within accretionary prism, Aleutian arc-trench system : 2D finite element modeling

Handi Lu*

Abstract : A series of finite element models simulate the paleostress field in the accretionary prism at different stages during the Late Cretaceous accretion of Mesozoic melange belts (McHugh Complex and Iceworm melamges) in the Chugach convergent margin, central-south Alaska. The accretionary prism is assumed to be elastic continuum. The subduction of the Pacific plate beneath the North American plate and the underplating of the oceanic crust is subjected as the boundary condition. The first episode of the Late Cretaceous accretion is modeled with two types of accretionary wedge of different length and width. From the finite element modeling, at initiation stage of accretion the paleostress σ_1 is compressive and nearly horizontal and thrust faults develop as the Pacific plate subducts beneath the North American plate. The underplating of the oceanic crust reoriented the paleostress field in the prism. Normal faults develop at the base of the accretionary wedge. Strike-slip faults develop in the deep portion of the oceanic crust. The underplating process might cause the lateral crustal growth and thickening of the wedge. At late stages of accretion, the paleostress σ_1 is compressive and nearly vertical at the toe of the wedge as the Late Cretaceous accreted sediments are poorly consolidated. However σ_1 is compressive and nearly horizontal as the accreted sediments are well consolidated. The consolidation state of the Late Cretaceous acreted sediments reguates the paleostress distribution at the toe of the wedge. The fault development at initiate stages of the Late Cretaceous accretion would result in tectonic and stratal disruption within the accretionary prism and leads to the formation of melamge belts. The formation of the melange belts is relative with the subduction of the Pacific plate beneath the North American plate and the underplating of the oceanic crust.

Key words : *accretionary prism, Aleutian arc-trench system, finite element method, Late Cretaceous accretion, subduction, underplating.*

1. Introduction

The eastern Aleutian arc-trench system has been studied intensively during the last four decades since the great 1964 Alaskan earthquake. The Gulf of Alaska is tectonically one of the most active regions in the world. The convergent margin of the North American plate is one of a few margins where older accretionary history is extensively exposed on land and where crustal growth is still active. Along the Aleutian trench, the Pacific plate moves north-northwest at a rate of 5-7 cm/y relative to the North American plate as shown in Fig. 1 (Jacob, 1986).

Although the subduction along the southern Alaska margin has continued since Early Jurassic, the growth of the Kodiak segment of the continental margin has been dominated by two relatively short episodes of accretion or crustal growth. The first episode of accretion is in Late Cretaceous and the second in Early Eocene (Byrne, 1986 ; Byrne and Fisher, 1987).

Received 4 June 2002 ; accepted 16 January 2003
* Graduate School of Engineering and Science, University of the Ryukyus, Nishihara, Okinawa 903-0213

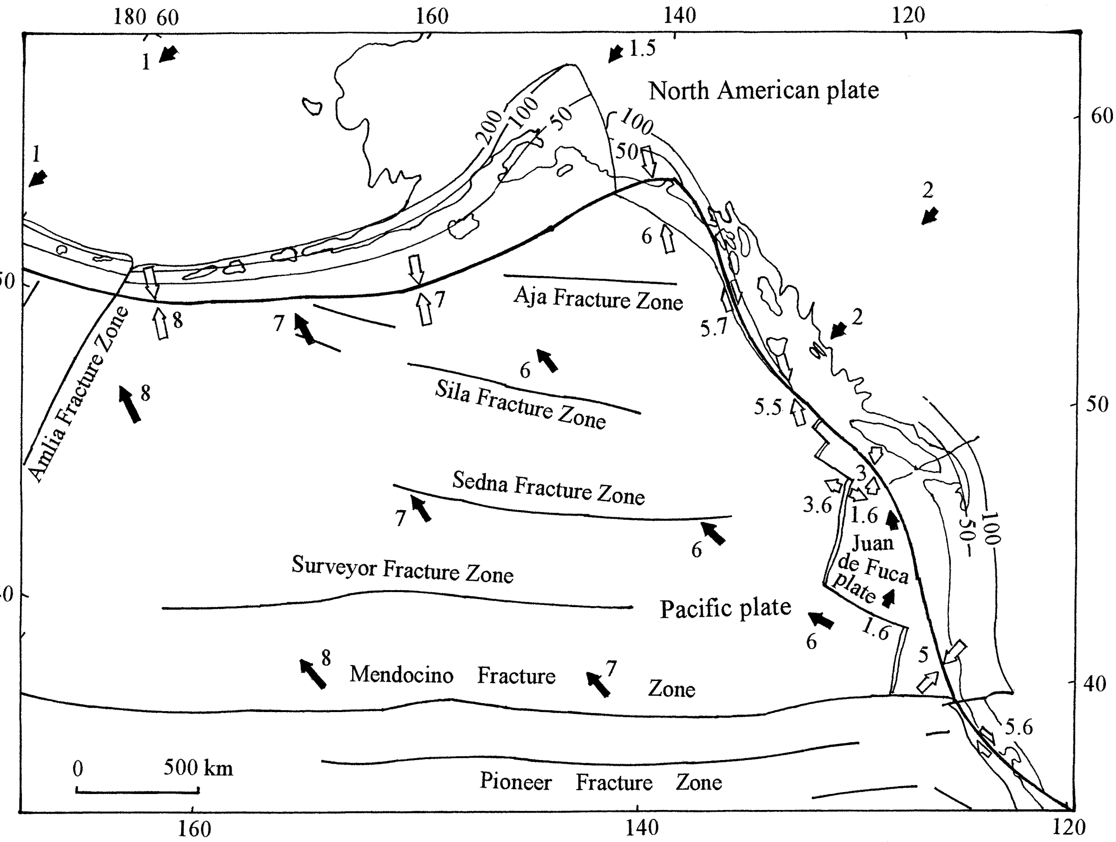

Fig. 1 Plate-tectonic map of the Gulf of Alaska showing the Pacific, North American, and Juan de Fuca plates, their absolute plate-motion vectors (solid arrows), and vectors of relative plate motions (open arrow). Isodepth contours of the deep seismic zone are displayed. Large numbers next to arrows indicate plate motion rates in cm/y (Jacob, 1986).

The finite element method is an effective tool to recover the regional paleostress field and deformation pattern if the structural and tectonic evolutionary history is clarified. Lundgren et al. (1995) used finite element modelling technique to study crustal deformation in Alaska arc-trench system. Hassani et al. (1997) proposed three finite element models (linear elastic, Maxwell viscoelastic and elastoplastic) to simulate plate deformation and stress during subduction process. Toth and Gurnis (1998) utilized a viscoelastic medium to study the dynamics of subduction initiation at preexisting fault zones in order to have a greater understanding of subduction process. Wang and Wang (1999) studied the kinematics and dynamics of the North American plate assuming a Newtonian rheology. Tang and Chemenda (2000) utilized the elastoplastic rheology to study the deformation and failure of the overriding plate during arc-continent collision in Taiwan.

In order to determine the deformation pattern of convergent margin within the accretionary prism, Aleutian arc-trench system, a numerical experiment is carried out with two-dimensional (2D) finite element method.

(1) The first episode of accretion or crustal growth in Late Cretaceous is modeled with two types of accretionary wedge of different length and width. The accretionary prism is simply treated as elastic continuum.

(2) A series of finite element models simulate the paleostress field in the accretionary prism at different stages of accretion. Fault developments is predicted according to the Mohr-Coulomb criterion. The subduction of the Pacific plate beneath the North American plate and the underplating of the oceanic crust is simplified to be the boundary condition. Increasing consolidation of the Late Cretaceous accreted sediments are taken into consideration by using different values of physical properties.

(3) The simulated results are compared with the deformation mechanism of melange formation by Moore and Byrne (1987), and the kinematic model of melange of the McHugh Complex by Kusky and Bradley (1999).

2. Geological setting

Alaskan Pacific margin is composed of two parallel composite terranes or 'superterranes'-the Wrangellian superterrane (consisting of the Peninsular, Wrangellia, and Alexander Terranes), and farther outboard, the Chugach-Prince William superterrane (Nokleberg et al., 1989, 1994 ; Plafker et al., 1994).

Chugach terrane in southern Alaska forms the outboard accretionary margin of the Wrangellian composite terrane, and consists of two major lithotectonic units, including Triassic-Cretaceous melange of the McHugh Complex and Late Cretaceous flysch of the Valdez Group (Kusky et al., 1997 b).

The McHugh Complex of central-south Alaska (Clark, 1973) and the Uyak Complex of Kodiak (Connelly, 1978), are melanges constituting part of the Chugach terrane (Fig. 2). It is interpreted as a Mesozoic-Cenozoic accretionary prism formed by offscraping (and/or underplating) outboard of the seaward margin of the composite Peninsular-Wrangellian-Alexander superterrane (Plafker et al., 1989 ; Bradley and Kusky, 1992 ; Kusky et al., 1997 a).

The Valdez Group is a less chaotically deformed flysch of argillite, and graywacke (Kusky et al., 1997 b). The Iceworm melange is interpreted as a contractional fault zone (Chugach Bay Thrust) along which the Valdez Group was emplaced beneath the McHugh Complex.

3. Description of finite element method

The finite element method is an extensively-used and helpful technique for numerical experiment of structural deformation in nature (Ramsay and Lisle, 2000). One example is the application of elastic rheological law under plane stress or plane strain condition. The elastic rheology, plane strain condition and prediction of fault development are discussed as follows.

3. 1. Elasticity : the elas.f code

Elastic materials deform when a force is applied and return to their original shape when the force is removed. In isotropic continuum the elastic properties are independent of direction. Turcotte and Schubert (1982) have pointed out that the upper half of the lithosphere is referred

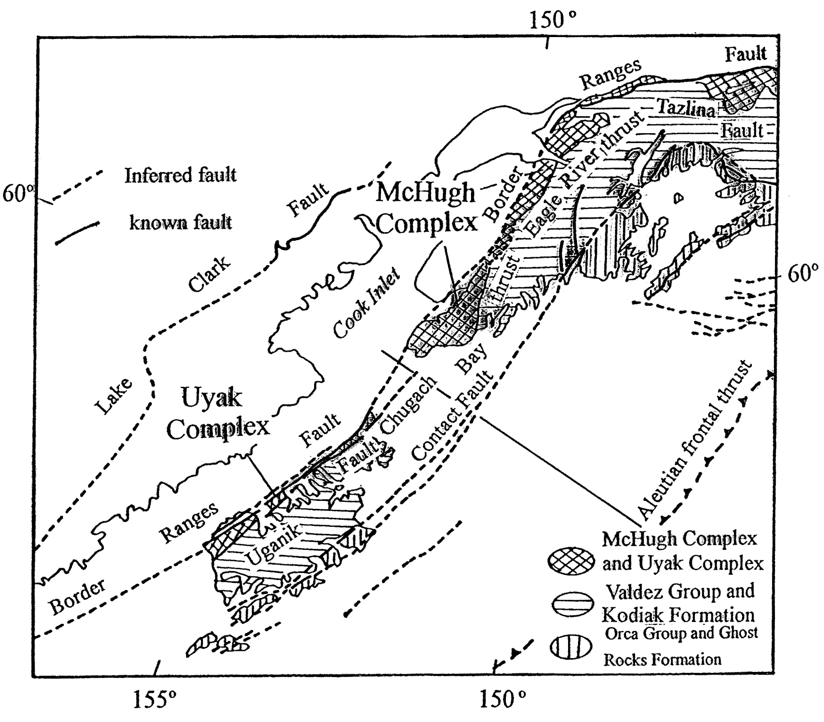

Fig. 2 Geological map of southern Alaska showing major tectonic elements (Kusky and Bradley, 1999).

to as the elastic lithosphere on the basis of the theory of plate tectonics. One of the fundamental postulates of plate tectonics is that the surface plates constituting the lithosphere do not deform significantly on geological time scales. Bott (1990) suggested that the uppermost 20 km of the continental crust was elastic, representing the strong and cool layer of the upper lithosphere. Hassani et al. (1997) also fixed the elastic thickness to 30 km for the oceanic lithosphere in their numerical models.

One important reason for studying the elastic behavior of the lithosphere is to determine the state of stress in the lithosphere. In this study linear elastic rheology is adopted under plane strain condition to recover the paleostress field in the accretionary prism during Late Cretaceous accretion in the eastern Aleutian arc-trench region. The paleostress field and fault development associated with the tectonic and stratal disruption which leads to the formation of melange structures can be simulated with numerical model in which treats the lithosphere as elastic, homogeneous and isotropic continuum. The elas.f code developed by Prof. D. Hayashi is used to calculate the displacements and stresses of finite element model. Gravitational body force is included in finite element models.

3. 2. Plane strain condition

The plane strain condition exists when there is one and only one zero component of principal strain. For example, the stain in a direction perpendicular to the x-y axis plane is zero, and none of the other two principal strains are zero.

Since the strike of tectonic units (Peninsular terrane, Chugach terrane) in the eastern Aleutian arc-trench system are nearly perpendicular to the convergent direction of the Pacific plate, the plane strain condition can be applied to simulate the paleostress field in the accretionary prism.

All the finite element models are in 2D elastic state under plane strain condition. The third principal stress σ^*, which acts over the section plane of the prism, can be obtained from the plane strain condition as

$$\sigma^* = \nu \cdot (\sigma_1 + \sigma_2) \qquad (1)$$

where ν is Poisson's ratio (Timoshenko and Goodier, 1970 ; Hayashi and Kizaki, 1972). According to the values of σ_1, σ_2 and σ^* of each finite element, the maximum, intermediate and minimum principal stresses are defined. The semi-3D stress field of each model is envisaged with the newly obtained principal stresses σ_1, σ_2 and σ_3.

3. 3 Prediction of fault development

As the semi-3D stress field of each model is available, it is possible to describe in which finite element a fault develops according to the Mohr-Coulomb criterion. The proximity to failure (PF) is calculated as the ratio of the current differential stress to the maximum differential stress predicted by the Mohr-Coulomb criterion (Melosh and Williams, 1989). Faulting occurs whenever the value of PF exceeds 1.0.

4. Models of accretion

A series of finite element models simulate for the paleostress field and fault development with different boundary conditions. σ_1 and σ_3 represent the maximum and minimum principal stress, and compression is taken as positive.

For the sake of simplification, Two critical tapers are applied for the accretionary wedge at different stages of the late Cretaceous accretion (see Moore et al., 1991). The oceanic crust is overlain by the accretionary wedge. The cross sections are oriented in NW-SE direction in the eastern Aleutian arc-trench region. The underplating of the oceanic crust along the base of the accretionary complex has played an important role in the Late Cretaceous accretion (Kusky and Bradley, 1997 b). The underplating process causes tectonic and stratal disruption within the accretionary prism. Rapid lateral accretion would cause the wedge to thicken to maintain the critical taper. The decollement dip of the accretionary wedge changes to be relatively gentle.

4. 1 Experiment I (initiation stage of accretion)

Models A1, A2 and A3 simulate for the paleostress field in the accretionary prism at initiation stages of the Late Cretaceous accretion as the Pacific plate subducts beneath the North American plate. The accretionary wedge in model A1 has a critical taper of 13° as shown in Fig. 3 a. It is about 90 km long and 20 km deep. The thick-

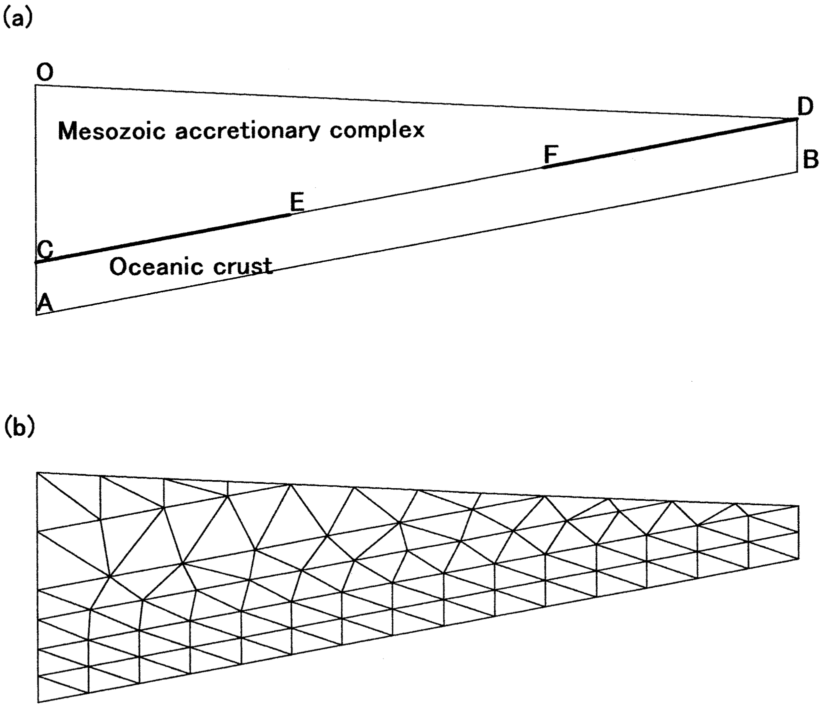

Fig. 3 (a) Model geometry of the Mesozoic accretionary wedge and oceanic crust at initiation stages of Late Cretaceous accretion, $\theta=13°$. (b) Finite element mesh of models A1, A2 and A3.

ness of the oceanic crust is 6 km. The dip of the oceanic crust is 10° to the horizon while the dip of the surface slope is 3°.

The finite element grid of models A1 consists of 83 nodes and 129 linear triangular elements (Fig. 3 b). The grid of models A2 and A3 is the same as model A1. As listed in Table 1, Young's modulus 70 GPa, Poisson's ratio 0.25 and density 2500 kg/m^3 are assigned to the accretionary complex, based on Clark (1996). Young's modulus 50 GPa, Poisson's ratio 0.25 and density 2800 kg/m^3 are assigned to the oceanic crust (see Condie, 1997).

The boundary condition of models A1, A2 and A3 is mentioned below. The left-side wall (OA) of the accretionary prism is horizontally constrained but vertically free. The convergent displacement, varing from the shallow node (700 m) to the deep node (160 m) with a decrement of 28 m, is subjected along the bottom of the oceanic crust (BA) in the three models. The convergent displacement of 700 m is subjected to the right-side wall of the prism (DB). Node A is fixed. The underthrusting of offscraped sediments is taken into account as the boundary condition in model A2. The underthrusting displacement of 700 m is subjected along the bottom of the overriding wedge (DF). The underplating displacement of 100 m is subjected along the interface (CE) between the accretionary complex and the oceanic crust in model A3 brcause the boundary between the oceanic crust and the overriding wedge is taken as free-slip condition.

The purpose for applying a varying convergent displacement in finite element models is to obtain a simulated result as that the paleostress σ_1 is nearly horizontal at the toe of the wedge. Hassani et al. (1997) proposed that the friction coefficient μ along the interface between two plates is a very important parameter for the stress regime of the overriding plate during the subduction process. If the friction coefficient μ increases from the shallow to deep portions along the subduction slope, the resistant force to the subduction of the underriding lithosphere increases greatly in the deep place. The subduction of the Pacific plate beneath the North American plate seems to be more difficult towards the deep place. It can be regarded as that the convergent rate along the subduction slope decreases from the shallow to the deep portion.

The semi-3D stress field of model A1 is illustrated in Fig. 4. σ_1 is compressive and nearly horizontal while σ_3 is compressive and nearly vertical. Cohesion strength 12 MPa and internal friction coefficient 1.0 are assigned to the accretionary complex and oceanic crust (Table 1).

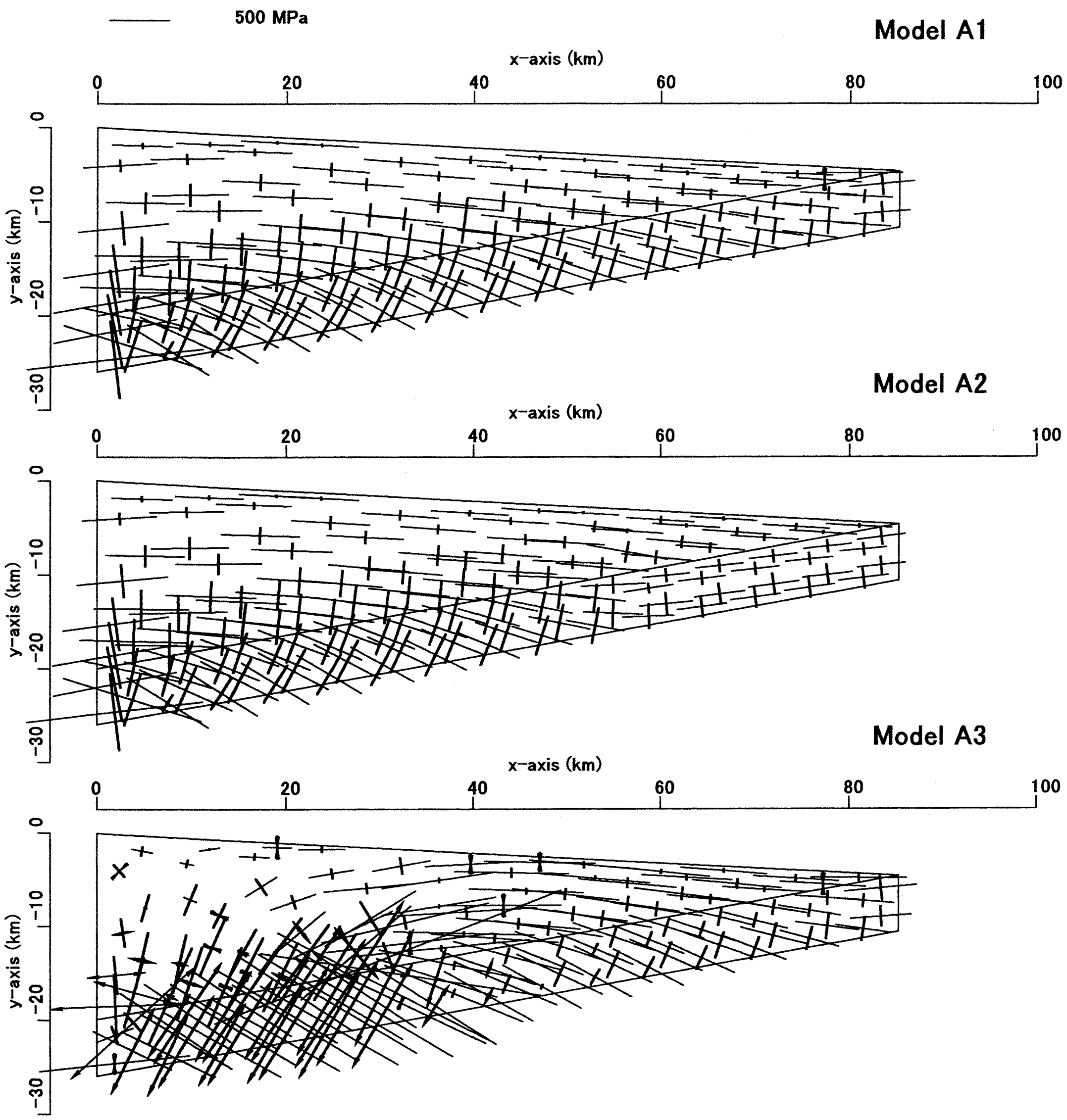

Fig. 4 Semi-3D stress field of models A1, A2 and A3, indicating magnitude and orientation of the principal stresses σ_1, σ_3. Straight lines represent compression, and lines with arrow represent tension.

As shown in Fig. 5 there are some finite elements with PF > 1.0 in the vicinity of the surface slope within the accretionary complex, where thrust faults develop.

The paleostress field of model A2 is similar to model A1 except that σ_1 is sub-parallel to the dip of the subduction slope within the shallow portion of the oceanic crust. Fault development in model A2 is similar to that in model A1.

The paleostress field of model A3 is different from model A1 in the deep portion of the accretionary complex and the oceanic crust. The paleostress σ_1 is reoriented to be oblique in the left half of the prism. And tensional stresses appear in the wedge and the oceanic crust. Fault development in model A3 is different from that in model A1. In model A3 thrust faults develop at the toe of the wedge and in some part of the oceanic crust. Strike-slip faults develop in the deep portion of the oceanic crust. Normal faults develop in the deep place of the accretionary complex.

The simulated results of experiment I are summarized as follows.

(1) The simulated results show that the paleostress σ_1 within the accretionary prism is compressive and nearly horizontal as the Pacific plate subducts beneath the North American

Table 1 Physical properties applied for different geological units.

Unit	Young's modulus (GPa)	Poisson's ratio	Density (kg/m^3)	Cohesion (MPa)	Coefficient
I	70	0.25	2500	12	1.0
II-1	5	0.20	2000	5	1.0
II-2	25	0.25	2050	8	1.0
II-3	60	0.25	2100	12	1.0
III	50	0.25	2800	12	1.0

Unit I: Mesozoic accretionary complex.

Unit II-1: accreted sediments (poorly consolidated).

Unit II-2: accreted sediments (half consolidated).

Unit II-3: accreted sediments (well consolidated).

Unit III: oceanic crust.

plate. Thrust faults develop at shallow place within the accretionary complex.

(2) The simulated results show that the underthrusting of offscraped sediments seems not influence the paleostress distribution of the wedge very much. However, the paleostress σ_1 is reoriented as being sub-parallel to the subduction slope in the shallow part of the oceanic crust.

(3) The simulated results show that the underplating of the oceanic crust reorients the paleostress axes and regulates fault development in the accretionary prism. Tensional stress appears and normal faults develop at deep place of the wedge. Strike-slip faulting occurs in the deep portion of the oceanic crust. Thrust faults develop at the toe of the wedge and in some part of the oceanic crust.

4. 2. Experiment II (late stage of accretion)

Models B1, B2 and B3 simulate for the paleostress field within the accretionary prism at late stages of the Late Cretaceous accretion. The accretionary wedge in model B1 has a critical taper of 10° (Fig. 6 a). It is 255 km long and 32 km deep. The oceanic crust is 6 km thick. The dip of the subduction slope is 7° to the horizon and the dip of the surface slope is 3°. The Late Cretaceous accreted sediments enclosed by quadrilateral EFDC is somewhat arbitrary (see Moore et al., 1991).

The finite element grid of model B1 has 190 nodes and 317 elements (Fig. 6 b). The grid of models B2 and B3 is the same as model B1. Physical properties assigned to the Mesozoic accretionary complex and the oceanic crust are the same in the three models. However different mechanic properties are applied to the Late Cretaceous accreted sediments of being poorly, half and well consolidated (Table 1).

The boundary conditions of models B1, B2 and B3 are the same as each other. The left-side wall (OA) of the accretionary prism is horizontally constrained but vertically free. The convergent displacement, varying from 700 to 37 m with a decrement of 14 m, is subjected along the bottom of the oceanic crust (BA). The convergent displacement of 700 m is subjected to the right-side wall of the prism (DB). Node A is fixed.

Model B1 simulates the paleostress field in the accretionary prism as the accreted sediments are poorly consolidated. Young's modulus 5 GPa, Poisson's ratio 0.20 and cohesion strength 5 MPa are adopted for the accreted sediments as being poorly consolidated (see Clark, 1966). The stress field of model B1 is shown in Fig. 7. Within the Mesozoic accretionary complex, σ_1 is

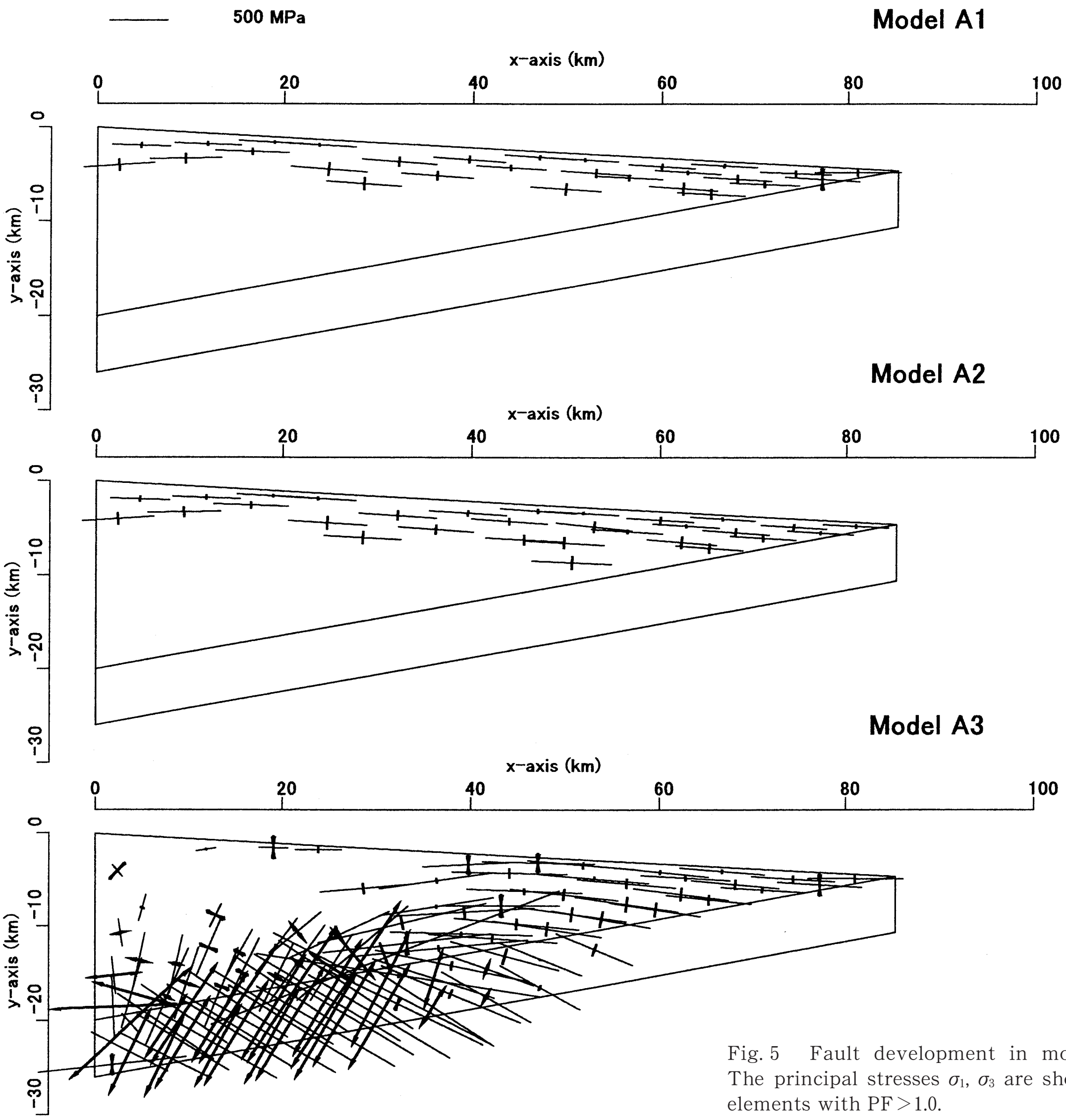

Fig. 5 Fault development in models A1, A2 and A3. The principal stresses σ_1, σ_3 are shown just for the finite elements with PF > 1.0.

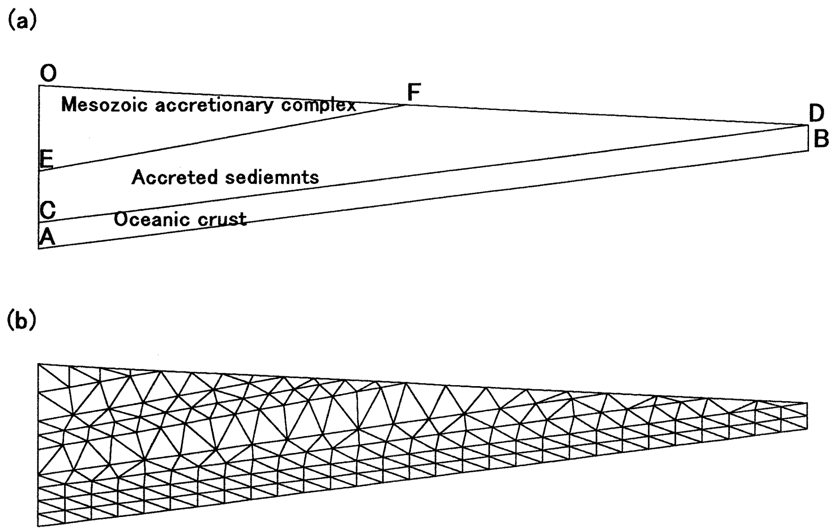

Fig. 6 (a) Model geometry of the Mesozoic accretionary wedge and oceanic crust at late stages of Late Cretaceous accretion, $\theta = 10°$. (b) Finite element mesh of models B1, B2 and B3.

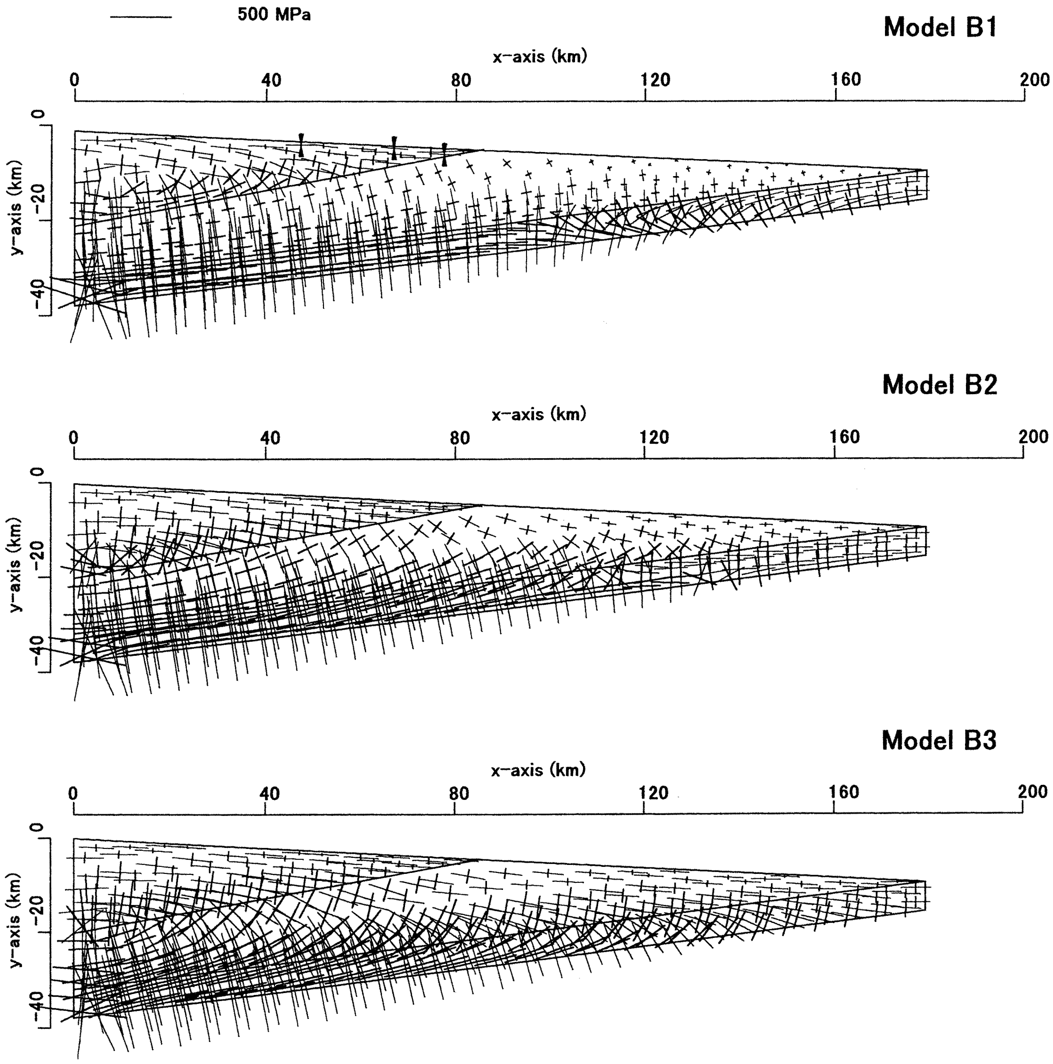

Fig. 7 Semi-3D stress field of models B1, B2 and B3, showing magnitude and orientation of the principal stresses σ_1, σ_3. Straight lines indicate compression, and lines with arrow indicate tension.

compressive and nearly horizontal in the vicinity of the surface slope. Within the accreted sediments σ_1 is compressive and nearly vertical at the toe of the wedge. As illustrated in Fig. 8, there is no finite elements with PF > 1.0 in the accreted sediments and no fault development occurs.

Model B2 simulates the paleostress field in the accretionary prism as the accreted sediments are partially or haif-consolidated. Young's modulus 25 GPa, Poisson's ratio 0.25 and cohesion strength 8 MPa are assigned to the half-consolidated sediments (see Clark, 1966). Within the Mesozoic accretionary complex σ_1 is compressive and nearly horizontal (Fig. 7). Within the accreted sediments σ_1 is compressive and nearly horizontal in the vicinity of the surface slope. There are few finite elements with PF > 1.0 in the accreted sediments, where thrust faults develop (Fig. 8).

Model B3 simulates the paleostress field in the accretionary prism as the accreted sediments are well consolidated. Young's modulus 60 GPa, Poisson's ratio 0.25 and cohesion 12 MPa are assigned to the accreted sediments as being well consolidated (see Clark, 1966). The stress field of model B3 shows that σ_1 is compressive and nearly horizontal at the toe of the wedge (Fig. 7). There are some finite elements with PF > 1.0 at the toe of the accretionary wedge, where thrust faults develop (Fig. 8).

The simulated results in experiment II are summarized as follows.

(1) The simulated results show that the consol-

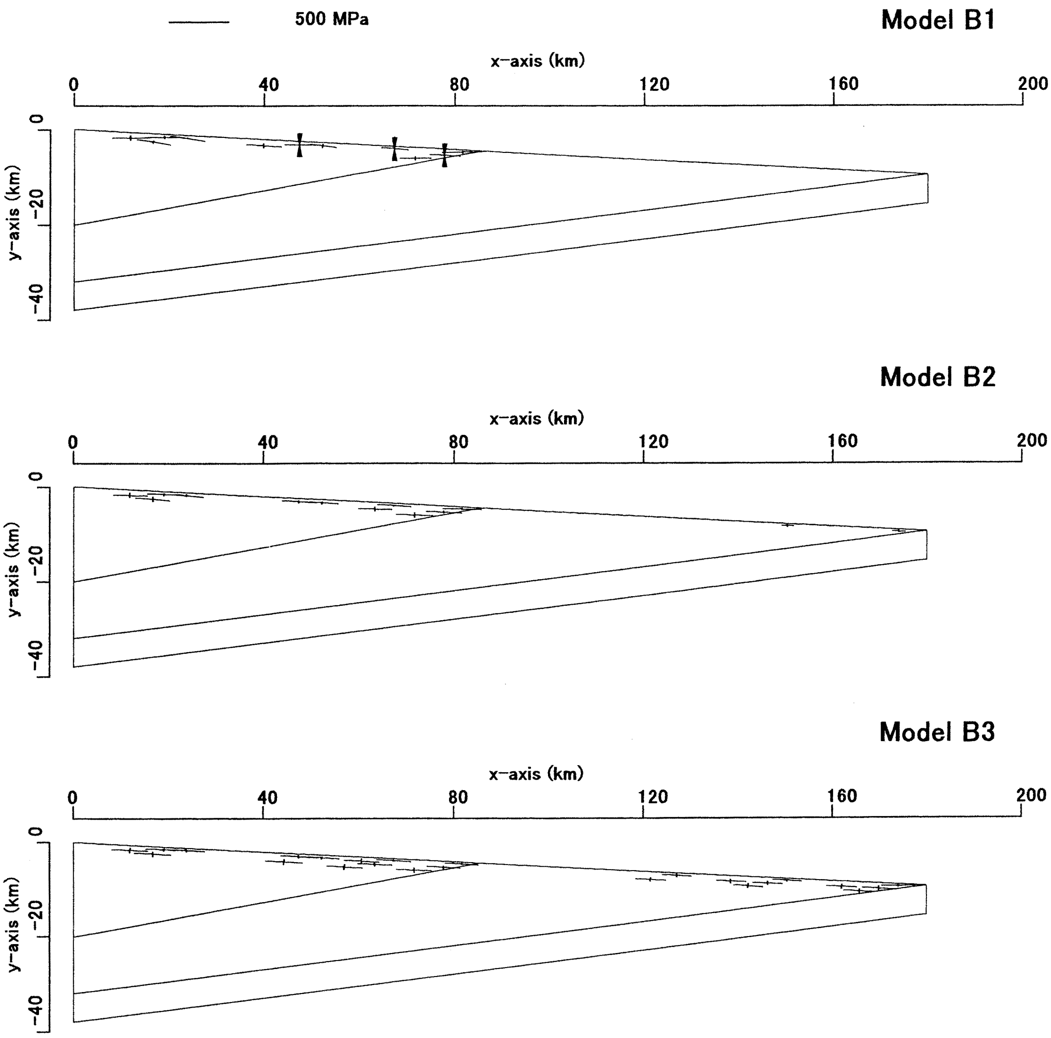

Fig. 8 Fault development in models B1, B2 and B3. The principal stresses σ_1, σ_3 are shown just for the finite elements with PF > 1.0.

idation state of the late Cretaceous accreted sediments regulates the paleostress distribution at the toe of the wedge. As the accreted sediments are poorly consolidated σ_1 is compressive and nearly vertical. However σ_1 is compressive and nearly horizontal as the accreted sediments are partially and well consolidate.

(2) The simulated results show that the consolidation state of the late Cretaceous accreted sediments controls the occurrence of thrust development at the toe of the wedge. No fault development occurs if the accreted sediments are poorly consolidated. In contrast thrust faults develop at the toe of the wedge as the accreted sediments are well consolidated.

5. Discussion

5.1. Comparison with Moore and Bynre's mechanism

The simulated results are in agreement with the mechanism of melange formation in accreting sediments-thickening of fault zones by Moore and Bynre (1987). In the opinion of Moore and Byrne (1987), sediments accreted at subduction zones undergo stratal disruption and form a type of melange (Fig. 9). The thickness of the disrupted zones grows with progressive deformation. Initial fault surfaces are abandoned and reorientation of fault surfaces occurs as deformation propagates into adjacent undeformed sediments. The disruption processes occurring

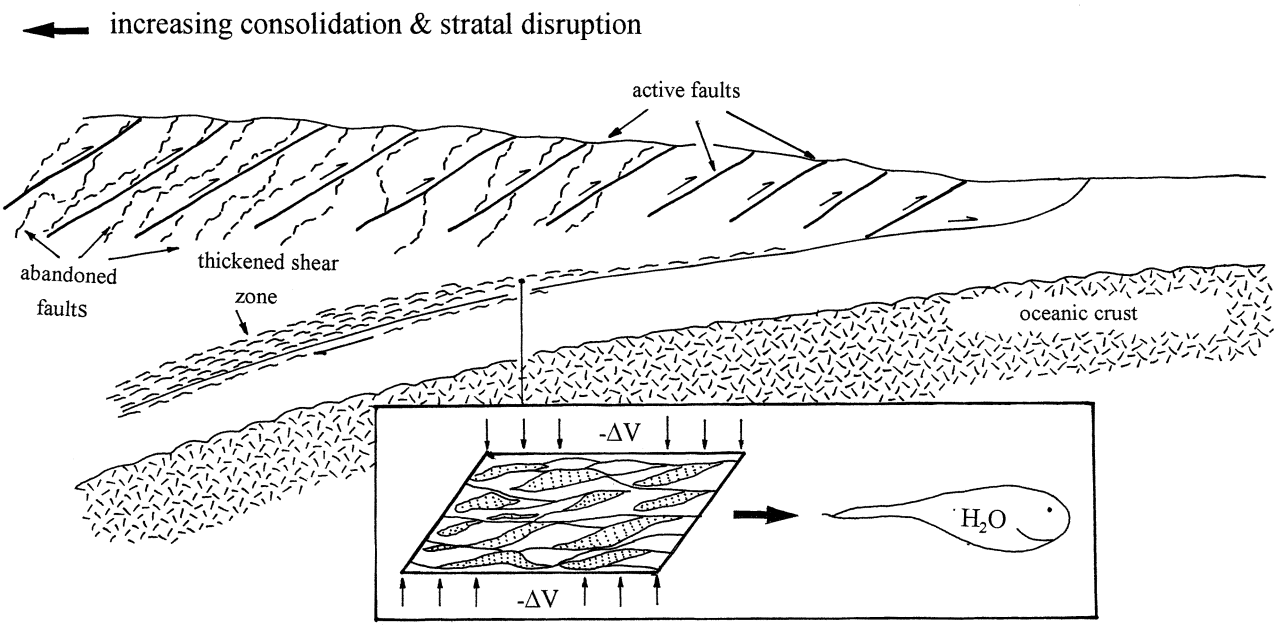

Fig. 9 Cross section of accretionary prism showing progeressive stratal disruption during offscraping and underthrusting (Moore and Byrne, 1987). In accreting sediments the initial fault surfaces are abandoned and deformation propagates into adjacent undeformed sediment.

in the accretionary wedge result principally from the deformation of the consolidating sedimentary mass. From the simulated results, the paleostress σ_1 is compressive and nearly horizontal and thrust faults develop at the toe of the accretionary wedge as the Pacific plate sbducts beneath the North American plate (Fig. 5). The fault development causes tectonic and stratal disruption in the accretionary complex and leads to the melange formation.

5. 2. Comparison with Kusky and Bradley's medel

The simulated results coincide with the schematic deformation medel of the McHugh Complex by Kusky and Bradley (1999). Firstly their schematic deformation model indicates that the paleostress σ_1 is slightly seaward-dipping to subhorizontal on a regional scale in the accretionary wedge (Fig. 10). The simulated results show that σ_1 is compressive and nearly horizontal at the toe of the wedge during the subduction process (Fig. 4). Secondly Kusky and Bradley (1999) proposed that melange of the McHugh Complex is generated by tectonic and stratal disruption at the toe of the accretionary wedge (Fig. 10). The simulated results show that faulting occurs in the accretionary wedge and the oceanic crust for the subduction of the Pacific plate beneath the North American plate and the underplating of the oceanic crust (Fig. 5). The fault development would cause tectonic and stratal disruption in the accretionary prism. The tectonic and stratal disruption is relative to the formation of melange structures in convergent margin.

5. 3. Underplating and accretion

The growth of the Kodiak segment of the continental margin has been dominated by two episodes of accretion, one in Late Cretaceous and the other in Early Eocene (Byrne 1986 ; Byrne and Fisher 1987). Two critical tapers with different length and thickness are applied to model the Late Cretaceous accretion in Chugach convergent margin. The oceanic plate is thinly sedimented at initiation stages of accretion but thickly sedimented at late stages of accretion.

During the Late Cretaceous accretion, the Pacific plate subducts beneath the North American plate. The paleostress σ_1 is compressive and nearly horizontal. Thrust faults develop in the accretionary complex. The Mesozoic rock layers are disrupted and offscraped at the toe of the wedge. The underthrusting of offscraped sediments does not greatly influence the paleostress

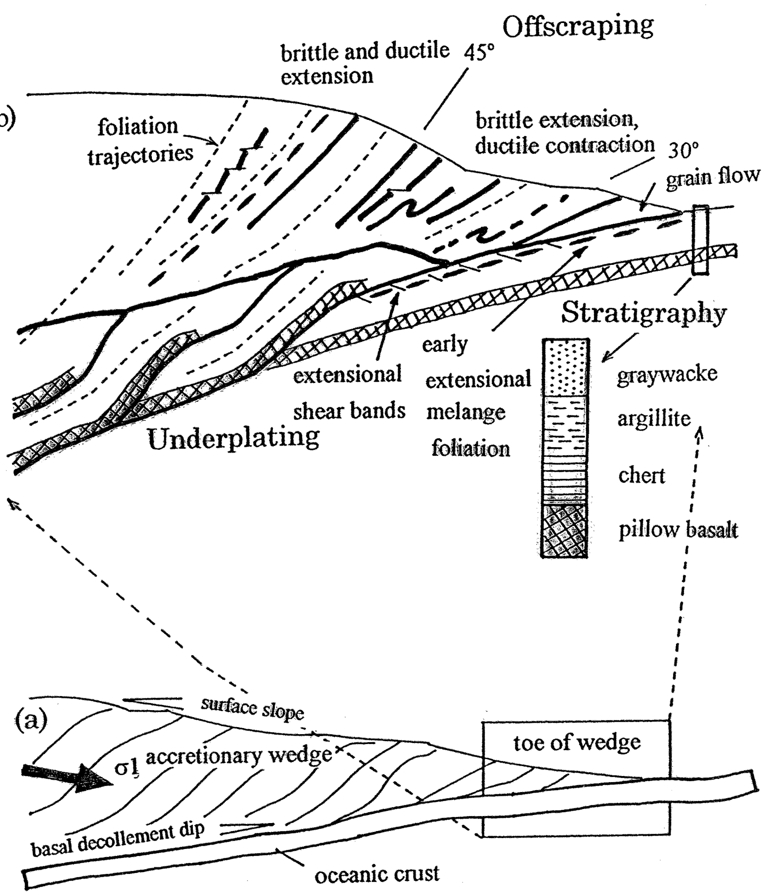

Fig. 10 (a) Schematic conditions of deformation in an accretionary wedge where σ_1 is slightly dipping to subhorizontal on a regional scale. (b) Schematic graph shows the different rheological units in the rock sequence experiencing both brittle and ductile extension (layers > 45° to σ_1), brittle extension and ductile contraction (layers 30–45° to σ_1), and dominantly brittle and ductile contraction (layers < 30° to σ_1). Early extensional melange formation at a low angle to σ_1 is related to sub-simple shear (Kusky and Bradley, 1999).

field in the accretionary prism. However the underplating process has played a major role in the accretion of the prism. The underplating of the oceanic crust reorients the paleostress axes and regulates the fault development in the accretionary prism. It generates normal faults around the base of the accretionary complex and causes strike-slip faulting in the deep portion of the oceanic crust. As the sediments are accreted in the wedge, the thickening of the wedge would happen and the decollement dip of the wedge changes to be relatively gentle.

5.4. *Role of sedimentation and consolidation*

The most persistent question relative to melange formation is the roles of soft-sedimentary vstectonic process on disruption and mixing. At late stages of the Late Cretaceous accretion, the wedge is in a rapid depositional environment and the accreted sediments are poorly consolidated at initiation. The simulated results show that the paleostress σ_1 is compressive and nearly vertical at the toe of the wedge and no fault develops as the accreted sediments are poorly consolidated. However as the poorly consolidated sediments are dewatered and hardened and well consolidated, compressive σ_1 becomes nearly horizontal and thrust faults develop at the toe of the wedge.

The increasing consolidation of the accreted sediments regulates the orientation of paleostress axes and controls the occurrence of thrust development at the toe of the wedge as the Pacific plate subducts beneath the North American plate. The gravity force only can not result in faulting within the accretionary wedge if no convergent displacement is subjected as the boundary condition. From this point, the sedimentary process has played little role in the formation of melange belts within the accretionary prism.

6. Conclusion

A series of finite element models simulate the paleostress field and fault development in the accretionary prism during the Late Cretaceous accretion in the eastern Aleutian are-trench region. All the simulated results obtained from the numerical modeling are summarized below.

(1) The simulated results show that the paleostress field in the accretionary prism evolves during the Late Cretaceous accretion. At initiate stages of accretion, the paleostress σ_1 is compressive and nearly horizontal at the toe of the accretionary wedge for the subduction of the Pacific plate beneath the North American plate. The paleostress axes are reoriented to be oblique for the underplating of the oceanic crust. At late stages of accretion the paleostress σ_1 is compressive and nearly vertical at the toe of the wedge as the accreted sediments are poorly consolidated. However the paleostress σ_1 is compressive and nearly horizontal at the toe of the wedge as the accreted sediments are well consolidated.

(2) The simulated results show that thrust faults develops within the accretionary complex at initial stages of the Cretaceous accretion for the subduction of the Pacific plate beneath the North American plate. The underplating of the oceanic crust generates normal faults around the base of the accretionary complex and strike-slip faults in the deep portion of the oceanic crust. At late stages fo the accetion no fault develops within the accreted sediments of being poorly cosolidated. However thrust faults develop at the toe of the wedge as the accreted sediments are well consolidated.

(3) The formation of melange belts in the convergent margin is relative to the subduction of the Pacific plate beneath the North American plate and the underplating of the oceanic crust. As the Pacific plate subducts beneath the North American plate, thrust faults developed within the accretionary complex. The underplating of the oceanic crust generates normal faulting around the base of the accretionary complex and strike-slip faulting and thrust development in the oceanic crust. The fault development causes tectonic and stratal disruption in the accretionary prism and leads to the formation of the McHugh Complex and Iceworm melange.

(4) The sedimentary process has played little role in the formation of melange belts in convergent margin. As the late Cretaceous accreted sediments are poorly consolidated and no faulting occurs at the toe of the accretionary wedge. However thrust faults develop within few finite elements with PF $>$ 1.0 at the toe of the wedge as the accreted sediments are well consolidated. The fault development and stratal disruption does not intensively occur within the accreted sediments. The consolidation process contributes less to the formation of melange belts in the accretionary prism.

Acknowledgements

The author gratefully acknowledges the Ministry of Education, Culture, Sports, Science and Technology, Japan for the support of Monbusho scholarship during his study period at University of the Ryukyus, Okinawa. Prof. D. Hayashi is thanked for critically reviewing of the manuscript. Other anonymous reviewers are thanked for their comments improved the manuscript greatly.

References

Bott, M. H. P., 1990. Stress distribution and plate boundary force associated with collision mountain ranges. *Tectonophysics,* **182**, 193–209.

Bradley, D.C. and Kusky, T.M., 1992. Deformation history of the McHugh accretionary complex, Seldovia Quadrangle, south-central Alaska. *In* Bradley, D.C. and Ford, A. eds., *Geologic Studies in Alaska by the U.S. Geological Survey during 1990*. U.S. Geological Survey Bulletin 1999, pp. 17–32.

Byrne, T., 1986. Eocene underplating along the Kodiak Shelf, Alaska : Implications and regional correlations. *Tectonics,* **5**, 403–421.

Byrne, T. and Fisher, D., 1987. Episodic growth of the Kodiak convergent margin. *Nature,* **325**, 338–341.

Clark, S. P. JR., 1966. Handbook of Physical Constants, revised ed., 587 p. The Geological Society of America, INC.

Clark, S. H. B., 1973. The McHugh Complex of south-central Alaska. *U.S. Geological Survey Bulletin* 1372–D, D1–D11.

Condie, K. C., 1997. Plate Tectonics and Crustal Evolution, 4th ed., 282 p. Butterworth Heinemann, Oxford.

Connelly, W., 1978. Uyak Complex, Kodiak Island, Alaska-a Cretaceous subduction complex. *Geological society of America Bulletin* **89**, 755–769.

Hassani, R., Jongmans, D. and Chery, J., 1997. Study of plate deformation and stress in subduction processes using two-dimensional numerical models. *Journal of Geophysical Research,* **102** (B8), 17951–17965.

Hayashi, D. and Kizaki, K., 1972. Numerical analysis on migmatite dome with special reference to finite element method. *Journal of the Geological Society of Japan* **78**, 677–686.

Jacob, K.H., 1986. Seismicity, tectonics, and geohazards of the gulf of Alaska regions. *In* Hood, D.W. and Zimmerman, S.T. eds., *The Gulf of Alaska, Physical Environment and Biological Resources*. U.S. Department of Interior, Minerals Management Service, pp. 145–184.

Kusky, T.M., Bradley, D.C., Haeussler, P., 1997 a. Progressive deformations of the Chugach accretionary complex, Alasuka, during a Paleogene ridge-trench encounter. *Journal of Structural Geology* **19**, 139–157.

Kusky, T.M., Bradley, D.C., Haeussler, P.J. and Karl, S., 1997 b. Controls on accretion of flysch and melange belts at convergent margins : Evidence from the Chugach Bay thrust and Iceworm melange, Chugach accretionary wedge, Alaska. *Tectonics* **16** (6), 855–878.

Kusky, T.M. and Bradley, D.C., 1999. Kinematic analysis of melange fabrics : examples and applications from the McHugh Complex, Kenai Peninsula, Alaska. *Journal of Structural Geology* **21**, 1773–1796.

Lundgren, P., Saucier, F., Palmer, R. and Langon, M., 1995. Alaska crustal deformation : Finite element modeling constrained by geologic and very long baseline interferometry data. *Journal of Geophysical Research* **100** (B11), 22,033–22,045.

Melosh, H.J. and Williams, C.A.JR., 1989. Mechanics of Graben Formation in Crustal Rocks : A Finite Element Analysis. *Journal of Geophysical Research* **94** (B10), 13,961–13,973.

Moore, J.C. and Byrne, T., 1987. Thickening of fault zones : A mechanism of melange formation in accreting sediments. *Geology* **15**, 1040–1043.

Moore, J.C., Diebold, J., Fisher, M.A., Sample, J., Brocher, T., Talwani, M., Ewing, J., Huene, R. von, Rowe, C., Stone, D., Stevens, C. and Sawyer, D., 1991. EDGE deep seismic reflection transect of the eastern Aleutian arc-trench layered lower crust reveals underplating and continental growth. *Geology* **19**, 420–424.

Nokleberg, W.J., Plafker, G., Lull, J.S., Wallace, W.K. and Winkler, G.R., 1989. Structural analysis of the southern Peninsular, southern Wrangellia, and northern Chugach terranes along the Trans-Alaska Crustal Transect, northern Chugach Mountains, Alaska. *Journal of Geophysical Research* **94**, 4297–4320.

Nokleberg, W.J., Plafker, G. and Wilson, F.H., 1994. Geology of south-central Alaska. *In* Plafker, G. and Berg, H.C. eds., *The Geology of Alaska, Decade of North American Geology*, vol. G1, pp. 311–366. Geological Society of America Press, Denver, CO.

Plafker, G., Nokleberg, W.J. and Lull, J.S., 1989. Bedrock geology and tectonic evolution of the Wrangellia, Peninsular, and Chugach terranes arong the Trans-Alaska Crustal Transect in the Chugach Mountains and southern Copper River Basin, Alaska. *Journal of Geophysical Research* **94**, 4,255–4,295.

Plafker, G. and Berg, H.C., 1994. Overview of the geology and tectonic evolution of Alaska. *In* Plafker, G. and Berg, H.C. eds., *The Geology of North America, vol. G-1*, The Geology of Alaska, pp. 989–1021. Geological Society of America, Boulder, CO.

Ramsay, J.G. and Lisle, R.J., 2000. The Techniques of Modern Structural Geology, vol. 3 : Applications of Continuum Mechanics in Structural Geology, 1061 p. Academic Press, London.

Tang, J.-C. and Chememda, A.I., 2000. Numerical modelling of arc-continent collision : application to Taiwan. *Tectonophysics* **325**, 23–42.

Timoshenko, S.P. and Goodier, J.N., 1970. Theory of Elasticity, 3rd ed., 567 p. McGraw-Hill.

Toth, J. and Gurnis, M., 1998. Dynamics of subduction initiation at preexisting fault zones. *Journal of Geophysical Research* **103** (B8), 18053–18067.

Turcotte, D.L. and Schubert, G., 1982. Geodynamics : Applications of Continuum Physics to Geological Problems, 450 p. John Wiley and Sons.

Wang, S. and Wang, R., 1999. Joint inversion of the kinematics and dynamics of the North American plate. *Tectonophysics* **302**, 173–201.